

Pressure Falloff Analysis

FORGE Well 16A(78)-32, Stage 1 HF

Colorado School of Mines

Team: Kaveh Amini

Ilker Uzun

Balnur Mindygaliyeva

Advised by Dr. Kazemi

8/04/2022

Objective of This Research

The **objective** of this research is to understand the information content of the well stimulation data of FORGE Well 16A(78)-32. For instance, the Stage 1 step-rate test, a variant of the classic diagnostic fracture injection test (DFIT), contains valuable information about the success of well fracturing and the nature of resulting formation stimulation in the drainage volume of Well 16A(78). The analysis we have provided is based on the classic pressure transient analysis in petroleum reservoirs. A most interesting aspect of FORGE data is its high quality. The next step in the analysis is to use the information we have discovered in the analysis of tracer flowback data.

This set of **slides** we have provided includes the pressure falloff analysis of the data recorded during stimulation of Stage 1 in injection Well 16A(78)-32 conducted in April of 2022. To honor multiple rate a superposition approach for linear flow regime was applied. The analysis yielded a permeability two orders of magnitude larger than permeability from cores. Our calculated permeability is essentially the effective permeability of micro- and macro-fracture system in the stimulated volume of the Well 16A(78)-32. Another observation is that after using the classic G-function plot, no closure stress was observed. This could suggest that pre-existing natural fractures were reopened during stimulation and yet had no propensity to close in accordance with the poroelastic properties.

Idealization of Granitoid Formation After Stimulation

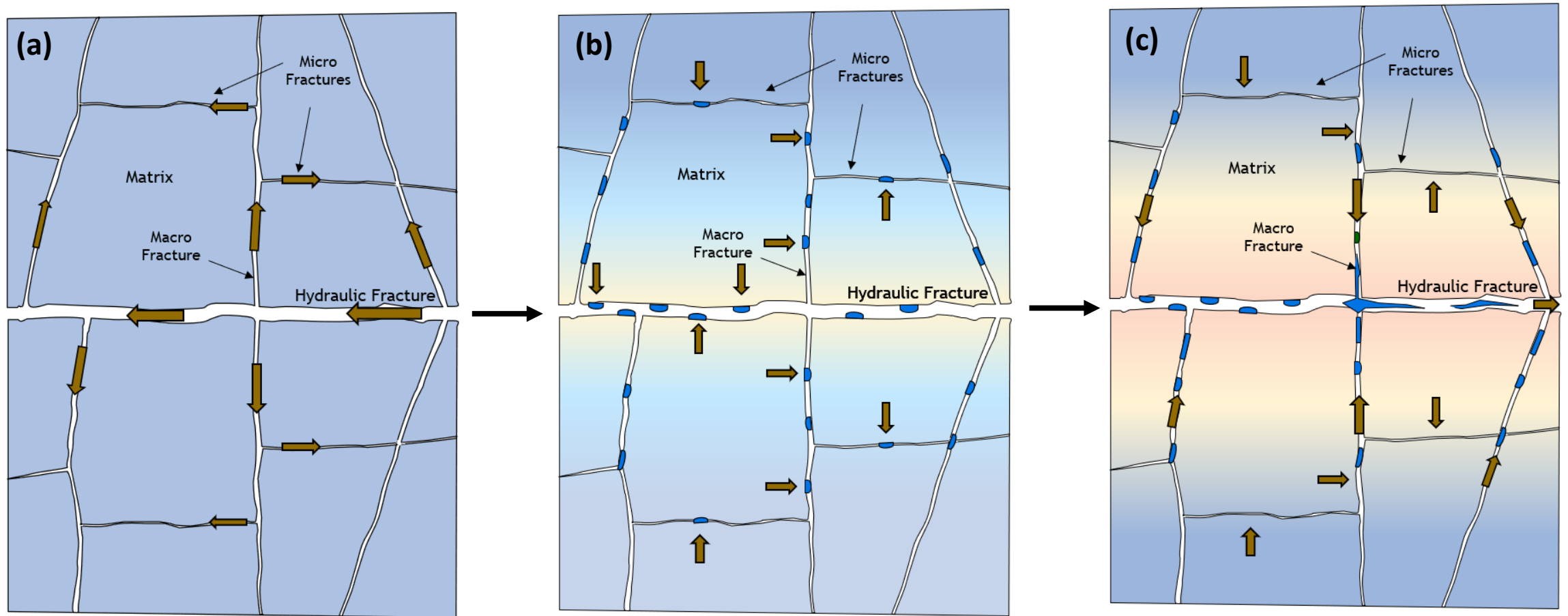
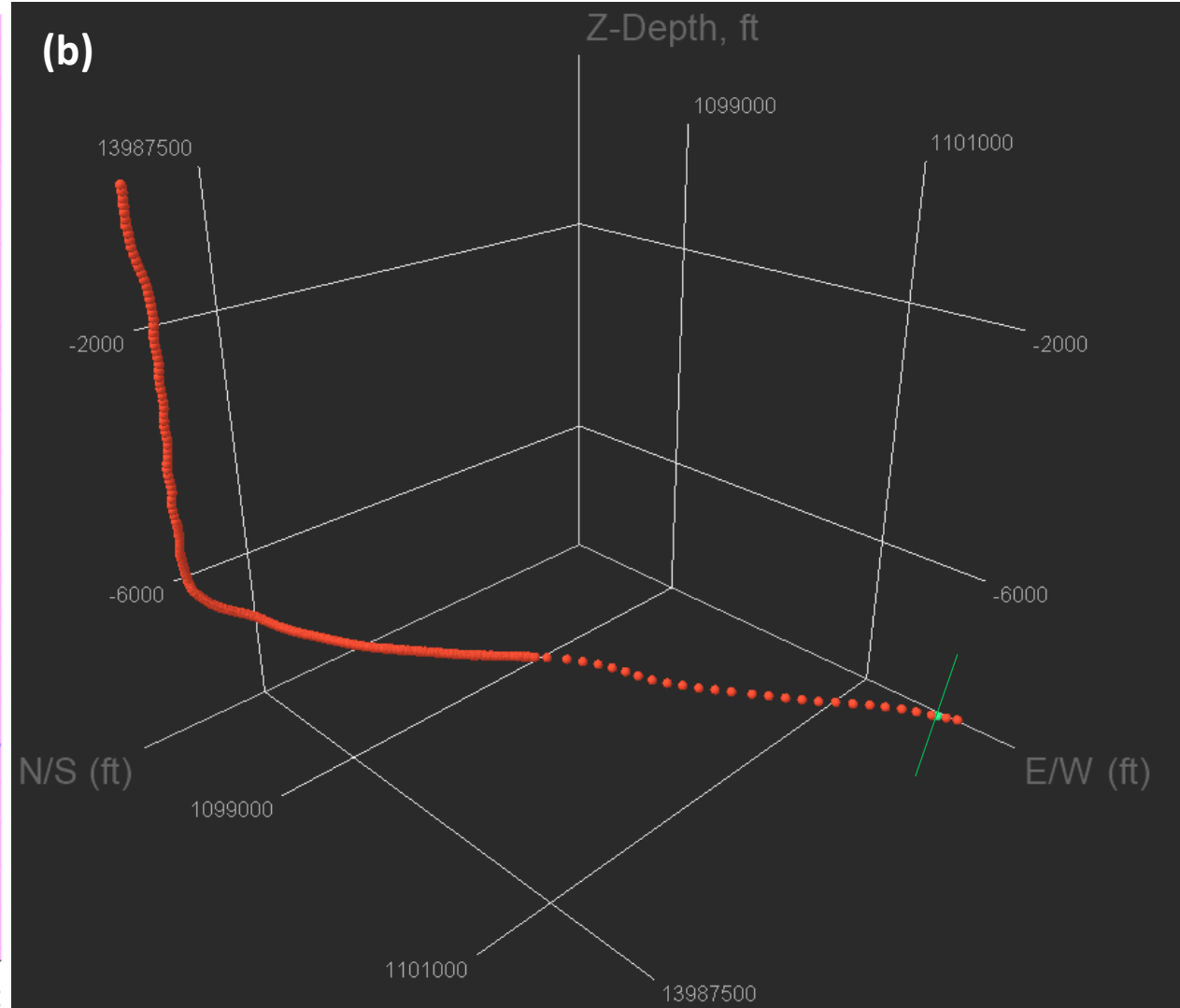


Figure 1. (a) Existing and induced fracture network; (b) water flows through stimulated micro- and macro-fractures to reach matrix; (c) water flows to the wellbore.

FORGE Well 16A(78)-32 – Directional Profile



Stage 1
 Open Hole Section
 10,826-10,828 ft MD
 68° to the vertical
 ~ 8512 ft TVD
 ~ 4327 BBL
 Green Line=Stage 1

Figure 2. (a) Directional profile (approximate elevation view)¹; (b) Plotted deviation survey in Spotfire

FORGE Well 16A(78)-32 – Analysis

1. Plot $p_{wf}(t_N + \Delta t)$ vs. $\sum_{j=1}^N \frac{q_j}{q_N} (\sqrt{(t_N + \Delta t) - t_{j-1}} - \sqrt{t_N + \Delta t - t_j})$ and identify the straight-line segment on the data plot.
1. The absolute value of the slope of the straight-line segment is $\frac{4.064 q_N \mu}{\sqrt{k}(hL_f)} \left(\frac{1}{(\phi c_t) \mu} \right)^{1/2}$.
2. The straight-line intercept at $\Delta t \rightarrow \infty$, we obtain a good estimate of initial reservoir pressure.
3. Fracture face damage or improvement is designated Δp_s which is equal to ***Injection pressure at shut in time – Formation extrapolated pressure from fall-off curve at $\Delta t = 0$*** . Use the following equation to calculate skin factor s_{hf}^{face} from: $\Delta p_s = \frac{141.2 q_N \mu}{kh} s_{hf}^{face}$.

FORGE Well 16A(78)-32 – Stage 1

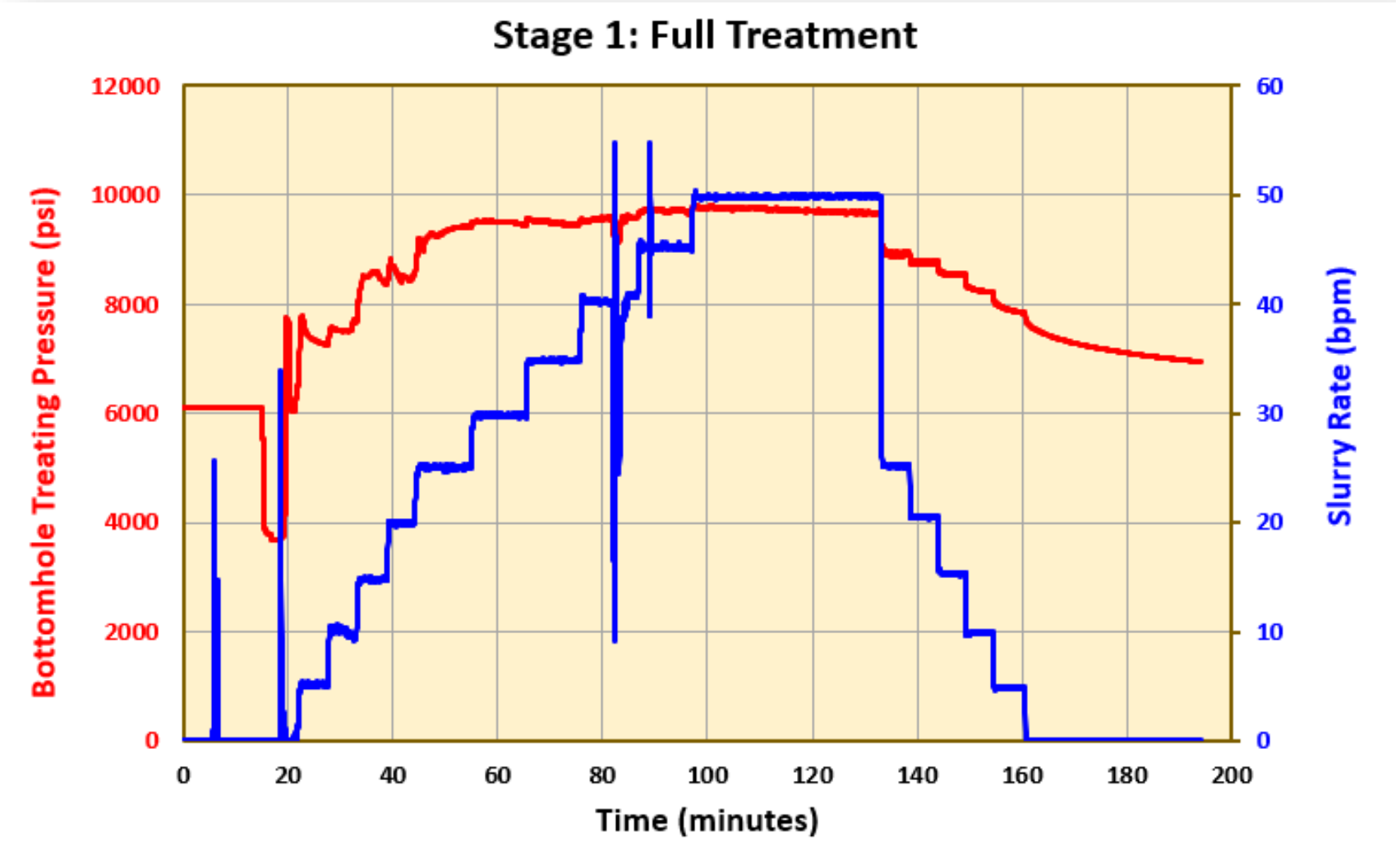


Figure 3.

FORGE Well 16A(78)-32 – Stage 1

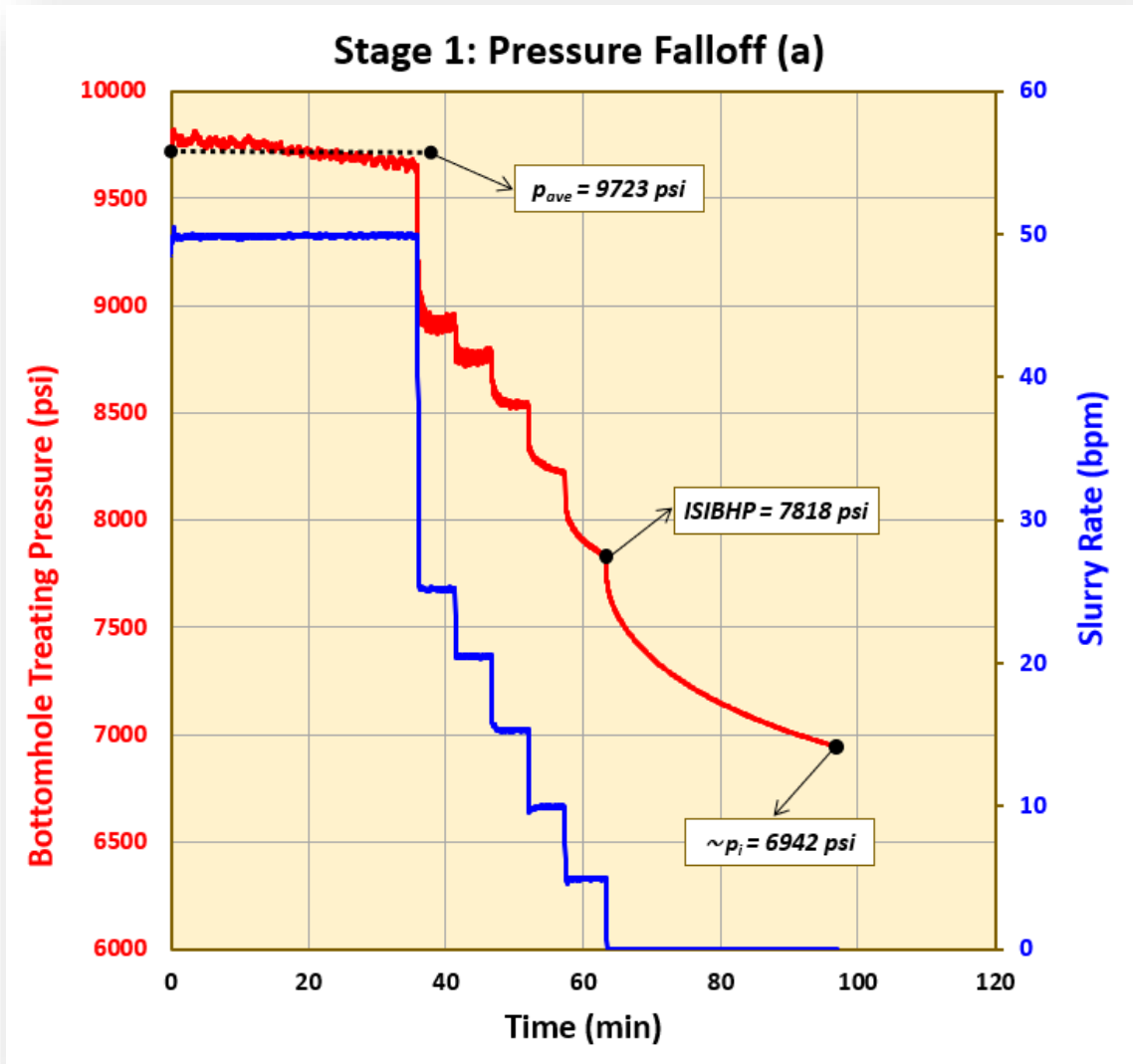


Figure 4(a).

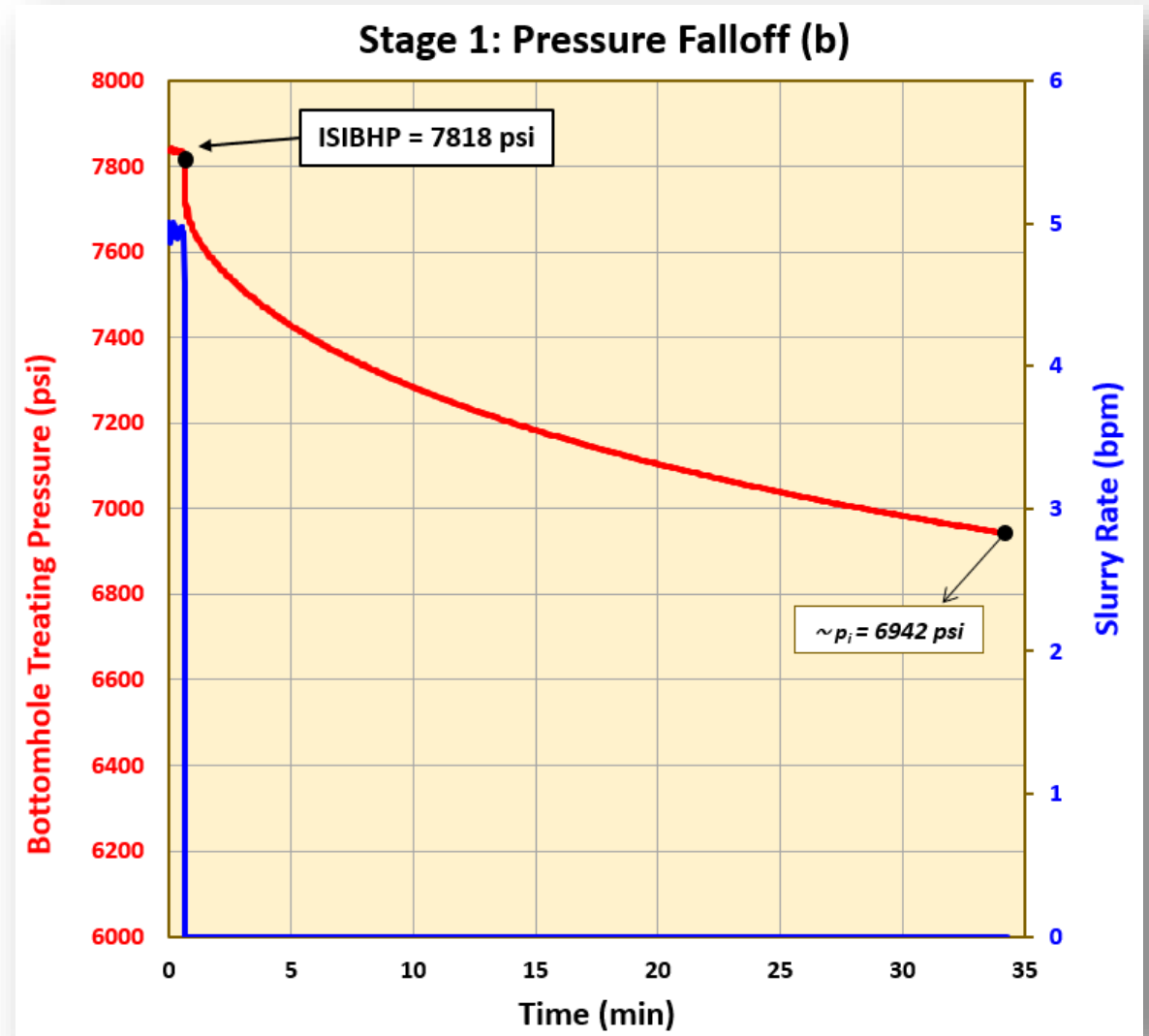


Figure 4(b).

FORGE Well 16A(78)-32 – Stage 1

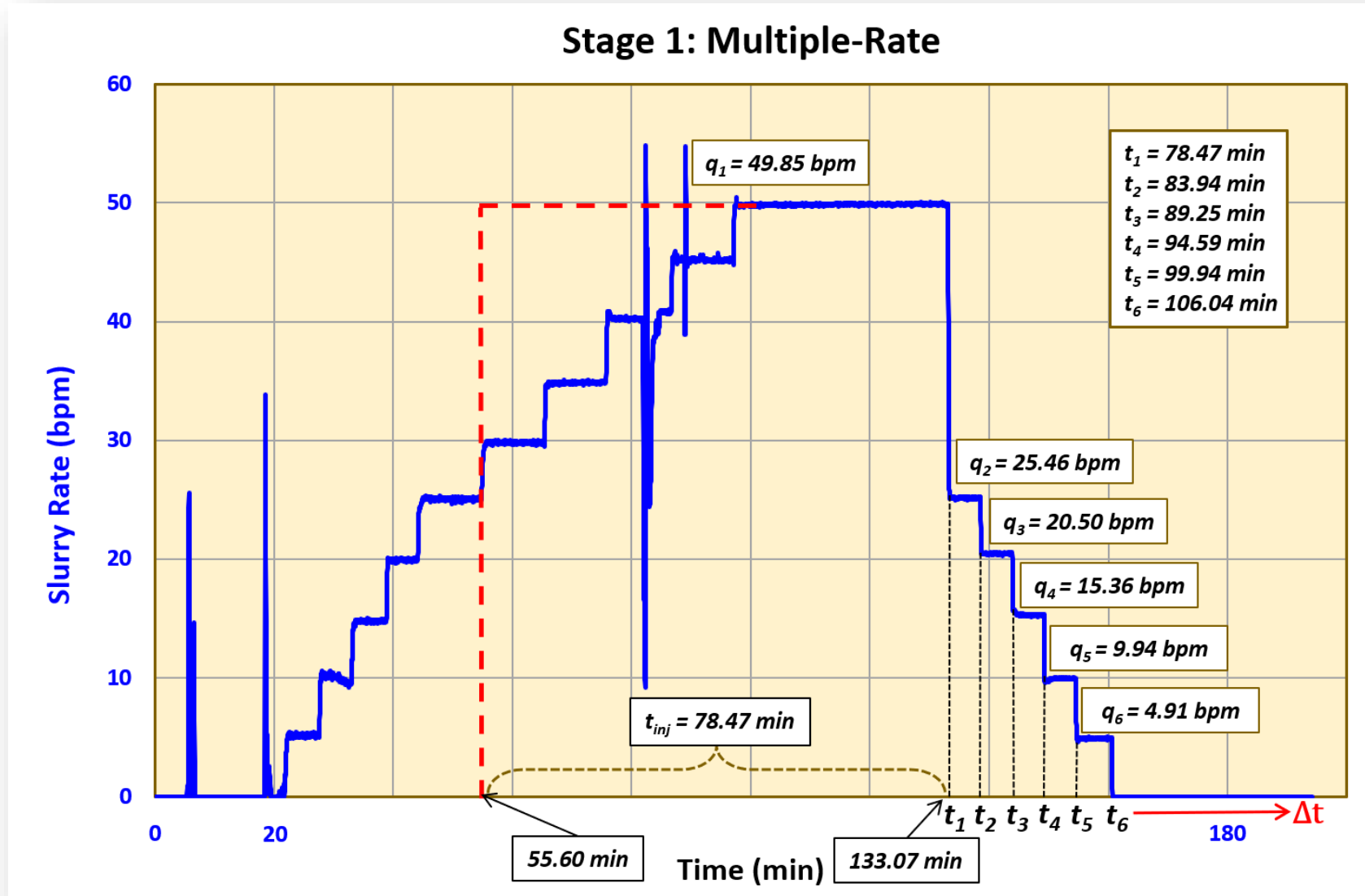
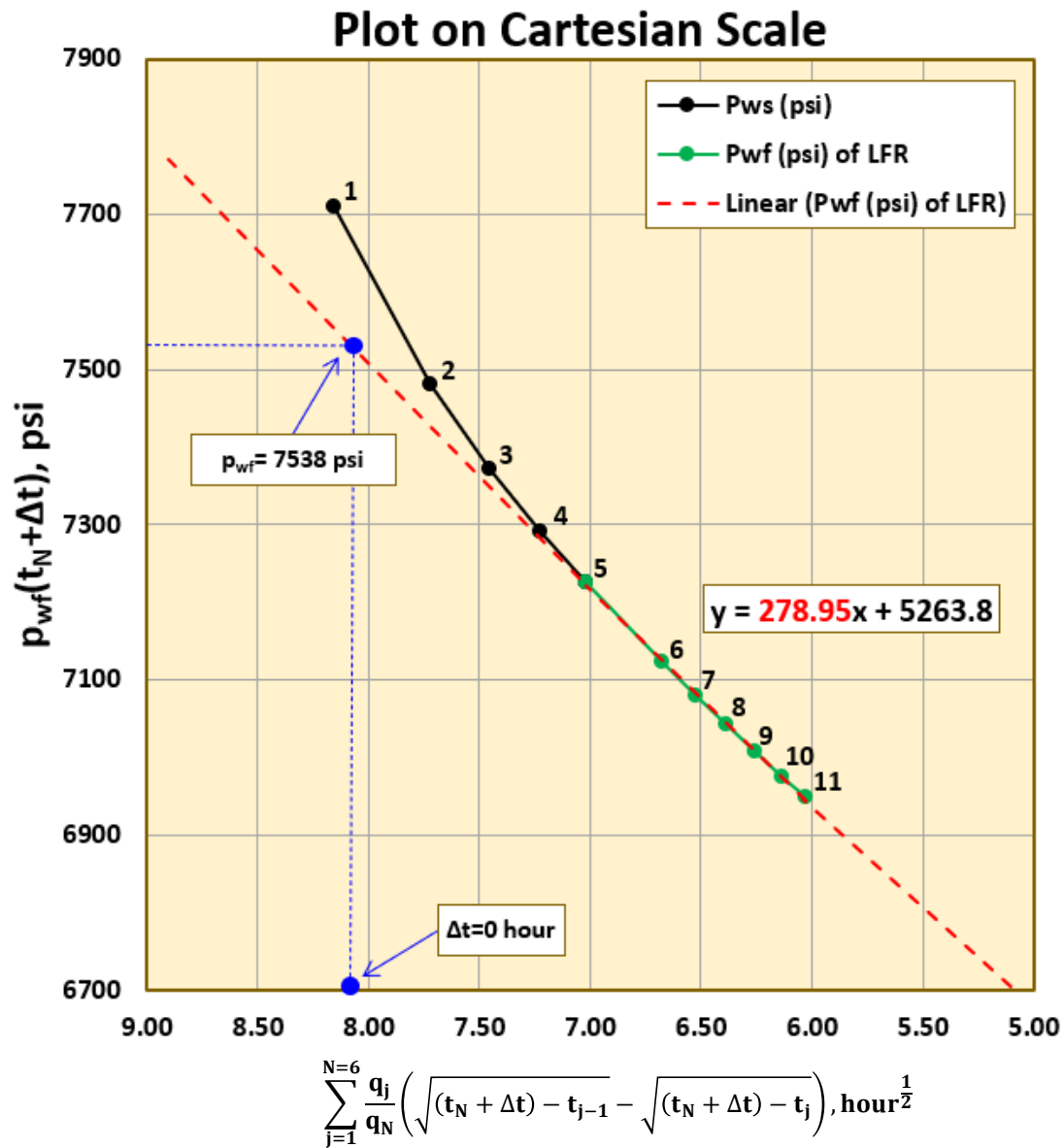


Figure 5.

FORGE Well 16A(78)-32 – Stage 1

Table 1. Tabulated Information from Figure 4

Designation	Time, min	Flow Rate, bbl/min	Time, hour	Flow Rate, bbl/day
q ₁	78.47	49.85	1.31	71784
q ₂	83.94	25.46	1.40	36662.4
q ₃	89.25	20.5	1.49	29520
q ₄	94.59	15.36	1.58	22118.4
q ₅	99.94	9.94	1.67	14313.6
q ₆	106.04	4.91	1.77	7070.4



#	Δt (min)
1	0
2	3
3	6
4	9
5	12
6	15
7	18
8	21
9	24
10	27
11	30

Figure 6.

Preliminary Results (1)

$$p_{w,f}(t_N + \Delta t) = p_i - \underbrace{\frac{4.064 q_N \mu}{\sqrt{k_{f,eff}}(hL_f)} \left(\frac{1}{(\phi c_t) \mu} \right)^{1/2}}_{\text{slope, } m} \left[\sum_{j=1}^N \frac{q_j}{q_N} \left(\sqrt{(t_N + \Delta t) - t_{j-1}} - \sqrt{t_N + \Delta t - t_j} \right) \right] \quad (1)$$

Parameter	Unit	Value
T^*	°F (°C)	358 (181)
q	RB/D	7070.4
μ^{**}	cP	0.152
h^{***}	ft (m)	656 (200)
L_f^{***}	ft (m)	328 (100)
ϕ	-	0.0118
c_t	psi ⁻¹	6×10^{-6}
m	psi/hr ^{1/2}	278.95

$$m = \frac{4.064 q_N \mu}{\sqrt{k_{f,eff}}(hL_f)} \left(\frac{1}{(\phi c_t) \mu} \right)^{1/2}$$

$$\sqrt{k_{f,eff}} = \frac{4.064 q_B \mu}{m_l(hL_f)} \left(\frac{1}{(\phi c_t) \mu} \right)^{1/2}$$

$$k_{f,eff} = \left(\frac{4.064 q_N \mu}{m(hL_f)} \right)^2 \left(\frac{1}{(\phi c_t) \mu} \right)$$

$$k_{f,eff} = \left(\frac{4.064 \cdot 7070.4 \cdot 0.152}{278.95 \cdot 656 \cdot 328} \right)^2 \left(\frac{1}{0.0118 \cdot 6 \times 10^{-6} \cdot 0.152} \right)$$

$$k_{f,eff} = 0.492 \text{ mD}$$

* Near equilibrium temperature at the reservoir depth².

** Water viscosity at 358°F (181°C).

*** "The required fracture height growth for the base case is 200 m"³.

The effective permeability of micro- and macro-fractures is much larger than the permeability measured from cores

Plot on Cartesian Scale - Extended Time

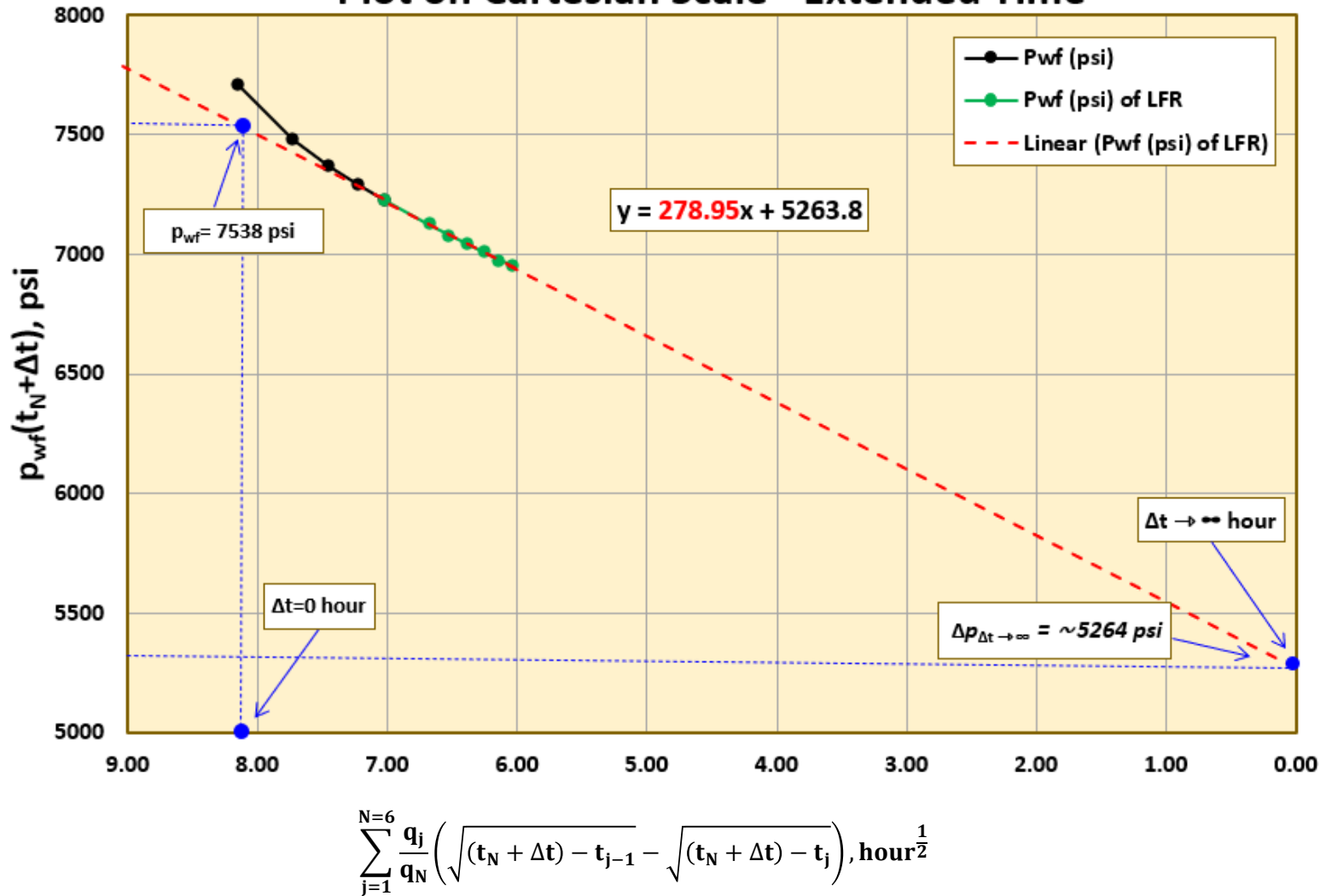


Figure 7.

Preliminary Results (2)

$$p_{\Delta t \rightarrow \infty} = 5264 \text{ psi}$$

$$p_R = 5264 \text{ psi}$$

$$ISIBHP - p_{wf, \Delta t=0} = \Delta p_{skin}$$

$$ISIBHP = 7818 \text{ psi}$$

$$\Delta p_{skin} = 7818 - 7538 = 280 \text{ psi}$$

$$\Delta p_{skin} = 280 \text{ psi}$$

Preliminary Results (3)

$$\text{Intercept} = \frac{141.2q_N\mu}{kh} S_{hf}^{face} = \Delta p_{skin} \rightarrow S_{hf}^{face} = \frac{\Delta p_{skin}kh}{141.2q_N\mu} \quad (3)$$

Parameter	Unit	Value
k	mD	0.492
q_N	RB/D	7070.4
B	RB/STB	1
μ	cP	0.152
h	$ft (m)$	656 (200)
Δp_{skin}	psi	280

$$S_{hf}^{face} = \frac{-280 \cdot 0.492 \cdot 656}{141.2 \cdot 7070.4 \cdot 0.152} = 0.596$$

$$S_{hf}^{face} = 0.596$$

Preliminary Results (4)

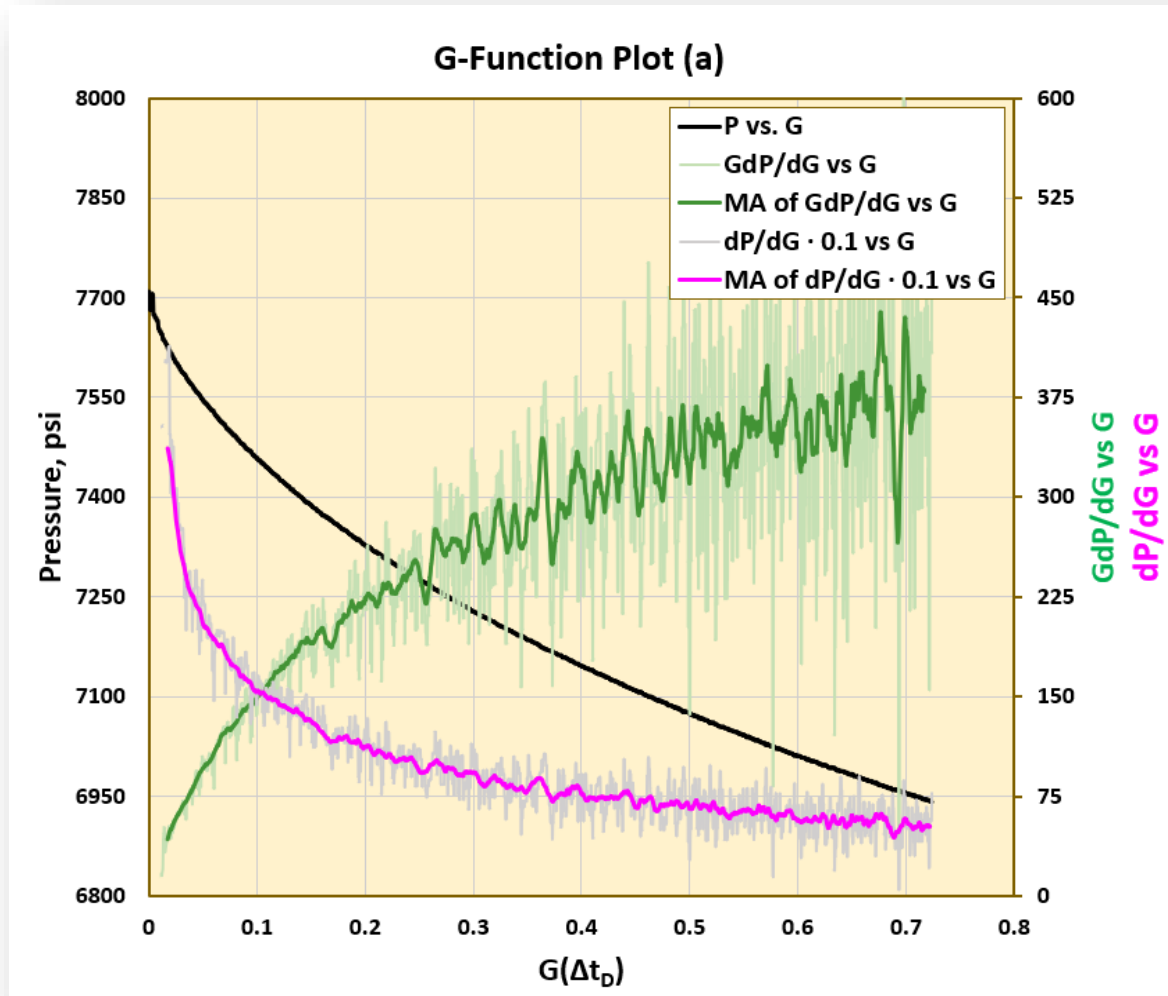


Figure 8(a). Continuous data.

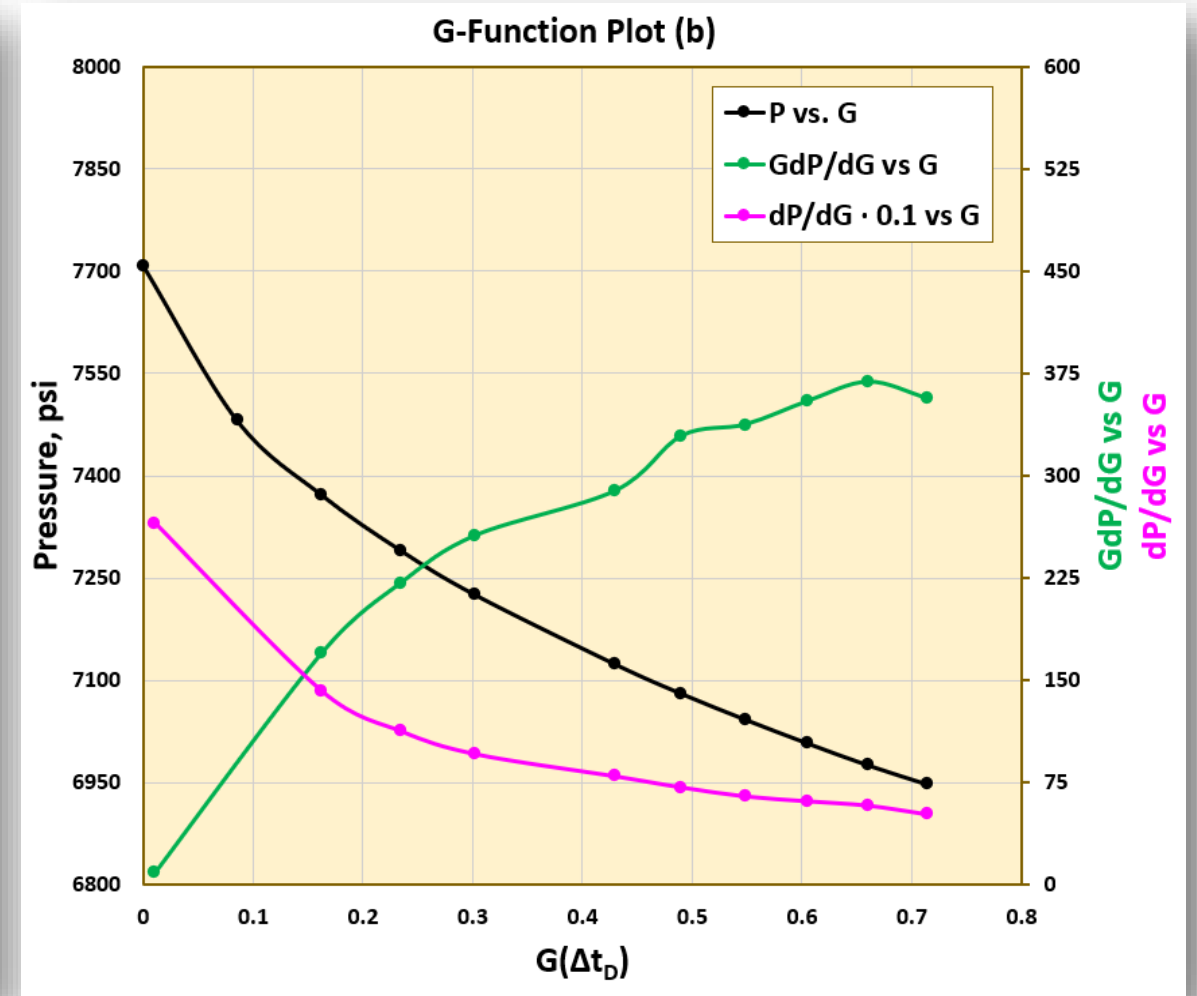


Figure 8(b). Discretized data.

Note: MA stands for moving average. dP/dG is divided by a factor of 10 for scaling purposes.

References

- [1] Winkler, D., Swearingen, L. (March 2021). Summary of Drilling Activities: Well 16A(78)-32
- [2] Allis, R., Gwynn, M., Hardwick, C., and Moore, J. (2018). The challenge of correcting bottom-hole temperatures – An example from FORGE 58-32, near Milford, Utah. Proceedings, 43rd Workshop on Geothermal Reservoir Engineering, Stanford University, Stanford, CA.
- [3] Nadimi, S., Forbes, B., Moore, J., Podgorney, R., & McLennan, J. D. (2020). Utah FORGE: Hydrogeothermal modeling of a granitic based discrete fracture network. Geothermics, 87, 101853. <https://doi.org/10.1016/j.geothermics.2020.101853>
- [4] England, K., McLennan, J., (May 2022). End of Job Report: Hydraulic Fracturing of Well 16A(78)-32 (April 2022).
- [5] Xing P et al.: In-situ stresses and fractures inferred from image logs at Utah FORGE. 2022
- [6] Zheng R et al: Heat extraction performance of a downhole coaxial heat exchanger geothermal system by considering fluid flow in the reservoir. 2018
- [7] Nadimi et al: DFIT and fracture modeling of the Utah FORGE site. GRC Transactions, Vol. 42, 2018
- [8] Nadimi, S., Forbes, B., Moore, J., Podgorney, R., & McLennan, J. D. (2020). Utah FORGE: Hydrogeothermal modeling of a granitic based discrete fracture network. Geothermics, 87, 101853. <https://doi.org/10.1016/j.geothermics.2020.101853>
- [9] Xing, P., McLennan, J., & Moore, J. (2020). In-Situ Stress Measurements at the Utah Frontier Observatory for Research in Geothermal Energy (FORGE) Site. Energies, 13(21). <https://doi.org/10.3390/en13215842>